

Feasibility study of biogas upgrading coupled with nutrient removal from anaerobic effluents using microalgae-based processes

E. Posadas¹, D. Szpak¹, F. Lombó², A. Domínguez³, I. Díaz³, S. Blanco⁴, P.A. García-Encina¹, R. Muñoz^{1*}

1.-Department of Chemical Engineering and Environmental Technology, University of Valladolid, Dr. Mergelina s/n. 47005, Valladolid (Spain), Phone: +34983186424; Fax: +34983184865.

2- IUOPA Research Unit “Biotechnology and Experimental Therapy based on Nutraceuticals- BITTEN”. Área de Microbiología. Departamento de Biología Funcional. Facultad de Medicina. Universidad de Oviedo. C/Julián Clavería, s/n. ES- 33006- Spain.

3- BIOGAS FUEL CELL S.A., Parque Tecnológico de Gijón, C\ Luis Moya 82, Edificio Pisa 1º izq, 33203 Gijón (Spain), Phone: +34984292020.

4- Department of Biodiversity and Environmental Management, University of León, 24071 León (Spain), Phone: +34987293139; Fax: +34987291563; (Current address: The Institute of the Environment. La Serna, 58, 24007 Leon, Spain).

*Corresponding author: mutora@iq.uva.es

ACKNOWLEDGEMENTS

This research was supported by Biogas Fuel Cell S.A and the Regional Government of Castilla y León (Project GR76, VA024U14 and RTA2013-00056-C03-02). A. Crespo, S. Santamarta, S. Arranz , J.M. Bueno, C. Mongil and G. Villamizar are gratefully acknowledged for their practical assistance.

ABSTRACT

The present research was conducted in order to simultaneously optimize biogas upgrading and carbon and nutrient removal from centrates in a 180 L high rate algal pond interconnected to an external CO₂ absorption unit. Different biogas and centrate supply strategies were assessed in order to increase biomass lipid content. Results showed 99% CO₂ removal efficiencies from simulated biogas at liquid recirculation rates in the absorption column of 9.9 m³ m⁻² h⁻¹, concomitant with nitrogen and phosphorus removal efficiencies of 100% and 82%, respectively, using a 1:70 diluted centrate at a hydraulic retention time of 7 days. The lipid content of the harvested algal-bacterial biomass remained low (2.9-11.2%) regardless of the operational conditions, with no particular trend over the time. The good settling characteristics of the algal-bacterial flocs resulted in harvesting efficiencies over 95%, which represented a cost-effective alternative for algal biomass reutilization compared to conventional physical-chemical techniques. Finally, high microalgae biodiversity was found regardless of the operational conditions.

Keywords: algal-bacterial symbiosis; biogas upgrading; biological wastewater treatment; microalgae lipid content; microalgae population dynamics.

Introduction

In the current global environmental and energy scenario, biogas upgrading coupled with nutrient removal from wastewaters in algal-bacterial photobioreactors constitutes a sustainable and promising alternative to conventional physical-chemical upgrading technologies (Bahr et al. 2014). This environmentally friendly and low energy demanding technology is based on the solar-powered photosynthetic fixation of CO₂ from biogas by microalgae. The *in situ* produced photosynthetic O₂ can be further utilized by sulfur oxidizing bacteria to oxidize the H₂S absorbed from biogas to SO₄²⁻, and by heterotrophic and nitrifying bacteria to oxidize the organic matter and nitrogen present in wastewaters to CO₂ and NO₃⁻, respectively (Bahr et al. 2014; Muñoz and Guieysse 2006).

On the other hand, the current high price of fossil fuels, together with their irreversible depletion and accumulation of greenhouse gases derived from their combustion, are nowadays promoting an intensive research on biofuels from sustainable biomass sources (Chisti 2007; Christenson and Sims 2011). First and second generation biodiesel entails severe limitations such as an extensive use of land (competing with human food crops) and costly pretreatments, respectively (Alam et al. 2012). In this context, biodiesel from microalgae constitutes a third generation biofuel able to overcome the above mentioned environmental and ethic limitations based on the high productivity of microalgal cultures, the possibility of using a low-quality water and the lack of competition with crop land (Ación et al. 2012). Biodiesel from microalgae is obtained from the transesterification of their lipids, whose content can range from 5 to 77% (on a dry weight basis) depending on the microalgal species and cultivation conditions (Chisti 2007). The high current cost monoalgal biomass cultivation (from 4.2 to 12.6 € Kg⁻¹ in 2010-2011) makes biodiesel from axenic microalgae non-competitive with conventional biodiesels, which requires a significant decrease in the biomass production costs (Ación et al. 2012; Norsker et al. 2011). The microalgae produced during the simultaneous upgrading of biogas and wastewater treatment constitutes a low cost and sustainable biomass feedstock for biodiesel production, since no fossil fuels-derived CO₂ is used (Ación et al. 2012; Bahr et al. 2014). High rate algal ponds (HRAPs) represent the most versatile and cost-effective photobioreactor platform for the simultaneous treatment of wastewater and upgrading of biogas (Bahr et al. 2014; Park et al. 2011). Unfortunately, this open photobioreactor configuration often undergoes contamination by native algae or zooplankton when sensitive microalgae are cultivated (De Godos et al. 2009; García et al. 2000; Park et al. 2011). Therefore, the year round predominance of lipid-rich microalgae in HRAPs seems unlikely based on the limited microalgae growth rates under lipid accumulation conditions (Breuer et al. 2012). In this context, nutrient deprivation has been shown as one of the most efficient strategies to induce storage lipid accumulation (Devi et al. 2013).

Despite the recent interest and intensive research conducted worldwide on microalgae cultivation as a promising technology for biofuel production, CO₂ mitigation and wastewater treatment, the number of experimental studies evaluating the performance of such an integrated process is scarce (Park et al. 2011; Serejo et al., 2015; Posadas et al., 2015). Thus, the main emphasis has been on pilot scale experiments focusing on biogas upgrading and wastewater treatment (Bahr et al., 2014; Heubeck et al., 2007). Serejo

et al. (2015) also evaluated the influence of the operational conditions in the chemical composition of the harvested biomass during the simultaneous biogas upgrading and wastewater treatment. In this study, we used a pilot-scale HRAP treating diluted wastewater centrate (the liquid fraction from the centrifugation of sludge digestate in sewage treatment plant) and CO₂ from biogas. CO₂ uptake was optimized under nutrient deprivation to enhance microalgae lipid accumulation. In addition, a morphological characterization of the microalgae assemblages was conducted.

Materials and methods

Microorganisms and culture conditions

The HRAP was initially filled with 0.75 g TSS L⁻¹ of a consortium of microalgae/cyanobacteria (henceforth referred to as microalgae) and bacteria treating diluted centrates (1:7) in a similar HRAP. The microalgae inoculum composition was (% of cells): *Microspora* sp. (53.5%), *Scenedesmus* (27.8%), *Synechocystis aquatilis* (13.9%) and *Woronichinia* sp. (4.7%). This microalgae population was selected based on its previous acclimation to the characteristics of the diluted wastewater. The population composition changed significantly over time (Tables S1-S7 Supplementary material).

Simulated biogas and centrate

The simulated biogas used was composed of CO₂ (30%) and N₂ (70%) instead of CH₄ in order to avoid any explosion hazards (Abello Linde, Spain). H₂S was not included, because of its complete removal reported by Serejo et al. (2015) regardless of the operational conditions. Centrate wastewater, which is characterized by a low biodegradable fraction and a high concentration of nutrients (Bahr et al., 2014; Posadas et al., 2013), was obtained from the digested sludge-concentrating centrifuges at Valladolid wastewater treatment plant (WWTP) (Spain) and stored at 4 °C prior to use. Centrate was diluted with tap water prior to feeding the HRAP in order to avoid microalgae inhibition due to its high NH₄⁺ concentrations and to control nutrient supply while compensating water evaporation losses (Table 1) (González et al. 2008). In a real case scenario, the use of the HRAP effluent (depleted from nutrients) as dilution water would significantly increase the economic and environmental sustainability of the process.

Table 1

Experimental set-up

The experimental set-up consisted of a 15 cm deep 180 L HRAP, with an illuminated surface of 1.33 m² (202 cm length × 63 cm width) and two water channels divided by a central wall, interconnected to a 2.5 L (Ø = 4 cm; height = 195 cm) external CO₂ absorption column (CO₂-AC) via microalgae broth external recirculation (Fig. 1). The CO₂ absorption unit consisted of a bubble column with a ceramic sparger located at its bottom. The system was operated indoors at the Department of Chemical Engineering and Environmental Technology (University of Valladolid, Spain) for 225 days at average temperature of 23±2°C. The HRAP cultivation broth was continuously mixed by a 6-blade paddlewheel at an internal recirculation velocity of approximately 20 cm s⁻¹. The surface of the HRAP was continuously illuminated

at $75 \pm 5 \mu\text{mol s}^{-1}\text{m}^{-2}$ of average irradiation using 15 Gro-Lux fluorescent lamps (Sylvania, Germany). Despite Shriwastav and Bose (2015) reported that intermittent illumination of 12-h light and dark periods at a light intensity of $246 \mu\text{mol m}^{-2} \text{s}^{-1}$ (\approx light saturation threshold for most microalgae species) was the most optimal strategy for sustainable algal-growth indoors, the continuous irradiation used in this particular research likely counterbalanced the low light irradiances used. Likewise, the successful results reported by Serejo et al. (2015) in a similar experimental set-up and at slightly higher light irradiances ($104 \pm 25 \mu\text{mol m}^{-2} \text{s}^{-1}$) and light:dark cycles of 16:8 h showed the sufficient microalgae-bacteria activity at the above mentioned light irradiation. Therefore, the low and continuous light irradiances here used did not invalidate the main outcomes and experimental findings of this study. Effluent sedimentation was carried out in a 8 L settler operated at 9 ± 1 h of hydraulic retention time (HRT) and located at the outlet of the HRAP (Bahr et al. 2014).

Figure 1

Operational conditions, sampling procedure and calculations

Six different operational conditions were tested in order to simultaneously optimize both CO_2 and nutrient removal from simulated biogas and diluted centrates, respectively, and the lipid content of microalgae. Based on these varied objectives, the achievement of an optimum microalgae growth along with the maximization of CO_2 removal in the AC and of lipid accumulation in the algal biomass was difficult. Therefore, the operational conditions were selected in order to obtain a balance for the target objectives. The HRT in the HRAP was maintained constant at 7 days during the entire experimental period, which corresponds to the optimum range for wastewater treatment in HRAPs (3-8 d) (Arbid et al. 2013; Posadas et al. 2015), while simulated biogas was sparged at $38.7 \pm 1.0 \text{ L d}^{-1}$ co-currently with an external recycling of algal cultivation broth drawn from the HRAP (at 1.1, 3.5 or $9.9 \text{ m}^3 \text{ m}^{-2} \text{ h}^{-1}$ or at their corresponding flow rate expressed in L d^{-1} of 34.8, 112.2 or 321.2 depending on the operational stage) (Fig. 1). The simulated biogas flow rate was chosen according to the results reported by Bahr et al. (2014) during the treatment of seven times diluted centrates at 23 d of HRT in a similar experimental set-up. Centrate dilution was maintained at 1:30 from stages I to IV and increased to 1:70 in stages V and VI in order to limit nutrient supply to the HRAP and to promote lipid accumulation due to the fact that nitrogen starvation has been reported as a successful strategy to increase the lipid content in microalgae cells (Toledo-Cervantes et al., 2013). The areal carbon, nitrogen and phosphorus loads supplied with the wastewater (and with the simulated biogas) ranged from 5.2 to $5.9 \text{ g C m}^{-2} \text{ d}^{-1}$, 0.2 to $0.6 \text{ g N m}^{-2} \text{ d}^{-1}$ and 0.02 to $0.05 \text{ g P m}^{-2} \text{ d}^{-1}$, respectively (Table 2). The pH of the cultivation broth, diffuser pore size in the absorption column and external liquid recirculation flow rate were modified throughout the different operational stages in order to increase the CO_2 mass transfer from the gas to the cultivation broth, and consequently the overall C/N/P ratio available for microalgae growth and lipid accumulation (Park et al. 2011). Thus, the pH of the cultivation broth was increased from 8.5 to 9.5 in stage II via automatic NaOH addition at 2% v/v (Table 2). Similarly, the pore diameter of the diffuser was decreased from 10 μm (porous glass diffuser) to 2 μm (metallic diffuser) in stage III. On the other hand, the external recirculation flow rate between the CO_2 -AC and the HRAP was maintained at $1.1 \text{ m}^3 \text{ m}^{-2} \text{ h}^{-1}$ in the first

three stages, and increased to $3.5 \text{ m}^3 \text{ m}^{-2} \text{ h}^{-1}$ in stage IV and V, and to $9.9 \text{ m}^3 \text{ m}^{-2} \text{ h}^{-1}$ in stage VI, which entailed an increase in the liquid/gas (L/G) recirculation ratio from 0.9 to 2.9 and 8.3, respectively (Table 2). All the tested conditions were maintained until the steady state was reached, which corresponded to ≈ 4 -5 times the elapsed HRT.

Table 2

Gas sampling (100 μL) was performed twice a week at the inlet and outlet of the CO_2 -AC in order to monitor CO_2 , O_2 and N_2 concentrations (Fig. 1). Similarly, the inlet and outlet gas flow rates were also measured to accurately determine CO_2 removal. Liquid sampling was also carried out twice a week by drawing 300 mL from the wastewater influent and effluent in the HRAP (Fig. 1) to monitor the concentrations of total organic carbon (TOC), inorganic carbon (IC), total nitrogen (TN), NH_4^+ , NO_2^- , NO_3^- , soluble phosphorus (P_s), total suspended solids (TSS), volatile suspended solids (VSS) and pH. Likewise, liquid samples of 300 mL were drawn from the cultivation broth twice a week to monitor IC, TSS and VSS concentrations. TOC, IC, TN, NH_4^+ , NO_2^- , NO_3^- and P_s concentrations corresponded to the soluble phase, and required liquid sample filtration through 0.20 μm nylon filters prior to analysis.

The parameters daily measured were ambient and cultivation broth temperatures, dissolved O_2 concentration (DO) in the cultivation broth and the influent and effluent wastewater flow rates, while light intensity at the HRAP surface was weekly monitored. Biomass harvesting was performed every 10 days by centrifugation of the biomass settled at the bottom of the sedimentation tank (Fig. 1).

The removal efficiency (RE) of CO_2 in the AC from the simulated biogas was quantified as follows:

$$\text{RE}_{\text{CO}_2} = \frac{C_{\text{CO}_2,\text{IN}} \cdot F_{\text{IN}} - C_{\text{CO}_2,\text{OUT}} \cdot F_{\text{OUT}}}{C_{\text{CO}_2,\text{IN}} \cdot F_{\text{IN}}} \cdot 100 \quad (1)$$

Where $C_{\text{CO}_2,\text{IN}}$ and $C_{\text{CO}_2,\text{OUT}}$ are the concentration (%) of CO_2 in the inlet and outlet biogas in the CO_2 -AC, respectively, while F_{IN} and F_{OUT} represent the inlet and outlet biogas flow rate (L d^{-1}), respectively. Likewise, the overall carbon removal efficiency was determined according to equation (2):

$$\text{RE}_C = \frac{(C_{\text{IN}} \cdot Q_{\text{IN}} + C_{\text{C-CO}_2,\text{IN}} \cdot F_{\text{IN}}) - (C_{\text{OUT}} \cdot Q_{\text{OUT}} + C_{\text{C-CO}_2,\text{OUT}} \cdot F_{\text{OUT}})}{(C_{\text{IN}} \cdot Q_{\text{IN}} + C_{\text{C-CO}_2,\text{IN}} \cdot F_{\text{IN}})} \cdot 100 \quad (2)$$

Where C_{IN} and C_{OUT} stand for the concentration of total dissolved C (TOC + IC) in the influent and effluent wastewater (mg L^{-1}), respectively, and Q_{IN} and Q_{OUT} for the influent and effluent wastewater flow rates in the HRAP (L d^{-1}). In this particular calculation, $C_{\text{C-CO}_2,\text{IN}}$ and $C_{\text{C-CO}_2,\text{OUT}}$ were expressed in $\text{mg C-CO}_2 \text{ L}^{-1}$.

TOC, IC, TN and P_s removal efficiencies were also estimated as follows:

$$\text{RE}_i = \frac{C_{i,\text{IN}} \cdot Q_{\text{IN}} - C_{i,\text{OUT}} \cdot Q_{\text{OUT}}}{C_{i,\text{IN}} \cdot Q_{\text{IN}}} \cdot 100 \quad (3)$$

Where $C_{i,\text{IN}}$ and $C_{i,\text{OUT}}$ correspond to, respectively, the influent and effluent concentrations (mg L^{-1}) of the target monitored parameter i (TOC, IC, TN or P_s).

The suspended solid removal efficiency of the settler (RE_{settler}) was calculated using the equation (4):

$$RE_{\text{settler}} = \frac{TSS_{\text{HRAP}} - TSS_{\text{effluent}}}{TSS_{\text{HRAP}}} \cdot 100 \quad (4)$$

Where TSS_{HRAP} and TSS_{effluent} stand for the TSS concentration (g TSS L^{-1}) in the HRAP and in the effluent, respectively. In this context, biomass productivity (W , $\text{g m}^{-2}_{\text{surface HRAP}} \text{d}^{-1}$) was quantified according to equation (5):

$$W = \frac{TSS_{\text{HRAP}} \cdot Q_{\text{out}}}{S} \quad (5)$$

where S represents the total HRAP illuminated surface.

Analytical procedures

The gas CO_2 , N_2 and O_2 concentrations were determined using a Varian CP-3800 gas chromatograph (Palo Alto, USA) equipped with a thermal conductivity detector, a CP-Molsieve 5A ($15 \text{ m} \times 0.53 \text{ mm} \times 15 \mu\text{m}$) and a CP-Pora BOND Q ($25 \text{ m} \times 0.53 \text{ mm} \times 15 \mu\text{m}$) columns. The concentrations of dissolved TOC, IC, and TN were measured using a Shimadzu TOC-VCSH analyzer (Japan) coupled with a TNM-1 chemiluminescence module. N-NH_4^+ concentration was determined with an NH_3 specific electrode Orion Dual Star (Thermo Scientific, The Netherlands). The concentrations of N-NO_3^- , N-NO_2^- and P-PO_4^{3-} were quantified by HPLC-IC according to De Godos et al. (2009). The concentration of soluble phosphorus was determined spectrophotometrically using the ammonium molybdate method (Spectrophotometer U-2000, Hitachi, Japan). All analyses, including TSS and VSS, were conducted based on Standard Methods (Eaton et al. 2005). The pH of the algal broth was on-line analysed using a R305 Consort system (Belgium), while a Eutech Cyberscan pH 510 (Eutech instruments, The Netherlands) was used for pH determination in the HRAP influent and effluent. Temperature and dissolved oxygen concentration were determined using an OXI 330i oximeter (WTW, Germany). The photosynthetic active radiation (PAR) was measured with a LI-250A light meter (LI-COR Biosciences, Germany).

The algal-bacterial biomass harvested in the settler was dried for 24 hours at $105 \text{ }^\circ\text{C}$ prior to characterization. The lipid content of the algal-bacterial biomass was determined gravimetrically following biomass extraction with a chloroform: methanol (2:1 v/v) solution (Kochert, 1978). The determination of the C and N content of the algal-bacterial biomass was conducted in a LECO CHNS-932 analyzer, while phosphorus content was determined spectrophotometrically after acid digestion in a microwave based on the internal procedure of the Instrumental Technical Laboratory of Valladolid University according to Standard Methods (Eaton et al., 2005). The identification, quantification and biometry measurements of the microalgae population were performed by microscopic examination (OLYMPUS IX70, USA) of biomass samples (fixed with lugol acid at 5% and stored at $4 \text{ }^\circ\text{C}$ prior to analysis) according to Sournia (1978).

Results

Temperature, evaporation losses and DO concentrations in the cultivation broth of the HRAP remained constant during the six operational stages (21-22 °C, 4-6 L m⁻² d⁻¹ and 6-8 mg O₂ L⁻¹, respectively) (Table 3).

Table 3

Stage I involved the start-up of the HRAP and was characterized by a RE_{CO₂} of 47±9% (Fig. 2).

Figure 2

Negligible RE_{TOC} were recorded in the HRAP both in stage I and in the rest of operational stages evaluated, despite effluent TOC concentrations remained low (ranging from 14 mg C L⁻¹ in stage I to 4 mg C L⁻¹ in stage V) (Table 3). The RE_{IC} and RE_C achieved during stage I (54±6% and 44±7%, respectively) represented the highest removal efficiencies along the 225 d of operation, and entailed the lowest IC concentration (47±6 mg C L⁻¹) in the cultivation broth. On the other hand, the RE_{TN} and RE_{Ps} were 99±1% and 74±7%, respectively, resulting in negligible nitrogen concentrations (0.3±0.3 mg L⁻¹) in the HRAP and in P-PO₄³⁻ effluent concentrations of 1.7±0.4 mg L⁻¹. N-NH₄⁺ was completely removed both in stage I and the rest of operational stages (Table 3).

The lowest biomass productivity, TSS concentration in the culture broth and RE_{settler} (1.3±0.2 g m⁻²d⁻¹, 0.11±0.06 g L⁻¹ and 66.4±4.0%, respectively) were recorded during this start-up period. The C, N and P content of the algal-bacterial biomass in stage I was 43.5%, 7.9% and 1.0%, respectively (Table 4).

Table 4

The predominant *Microspora* sp. present in the inoculum was gradually replaced by *Pseudanabaena minima* during stage I, which also coexisted with *Scenedesmus* and *Limnothrix mirabilis*, each representing 15% of the total population (Fig. 3).

Figure 3

The lipid content of the harvested biomass in stage I decreased from 7.4±2.1% (in the inoculum) to 4.6±2.8% (Table 4).

Once nitrogen was depleted in the cultivation broth under steady state I, the pH of the cultivation broth was increased from 8.5 to 9.5 in order to enhance CO₂ transfer from the biogas to the liquid phase in stage II, which entailed similar RE_{CO₂} to stage I (54±5%). Negative RE_{IC} were recorded from stage II onwards, which led to a significant IC concentration increase in the growth medium to 144 mg L⁻¹ in stage II (Fig. 2). Similarly, RE_C also decreased during stage II to 25±7% (Table 4). On the other hand, the RE_{TN} during stage II accounted for 66±7%, with TN effluent concentrations of 7±2 mg TN L⁻¹ (which corresponded to nitrate concentrations). RE_{Ps} in stage II decreased to 48±5%, with an effluent concentration of 1.4±0.3 mg L⁻¹ (Table 4). Biomass productivity and suspended solids concentration in the HRAP increased to 5.4±0.2 g m⁻² d⁻¹ and 0.39±0.10 g TSS L⁻¹, respectively, while RE_{settler} was 98.2±1.2%. C, N and P biomass content in stage II was 35.6%, 5.9% and 1.6%. During stage II, *Chroococidiopsis* sp. was the predominant microalgae in the HRAP, while *Microspora* sp. was again identified at similar abundances to

Synechocystis aquatilis (11.2% and 9.4%, respectively). The lipid content of the algal-bacterial biomass in stage II ($5.2\pm 2.1\%$) was similar to stage I.

A similar RE_{CO_2} ($48\pm 4\%$) to previous stages was recorded when decreasing the diffuser pore size in stage III in order to increase the mass transfer area, which was expected to bring about an enhanced RE_{CO_2} according to Fick's equation $D = K_a \cdot a \cdot \Delta C$ (Bird et al. 2006). The RE_C in this stage was $20\pm 4\%$, while IC concentration in the HRAP remained similar to the previous stage. The RE_{TN} decreased to $40\pm 2\%$, which entailed the highest TN concentrations in the HRAP broth ($21\pm 2 \text{ mg L}^{-1}$), while RE_{P_s} remained constant at $51\pm 5\%$, resulting in P_s concentration of 2 mg L^{-1} . Biomass productivity and concentration in the algal pond decreased in stage III to $3.9\pm 0.9 \text{ g m}^{-2} \text{ d}^{-1}$ and $0.25\pm 0.06 \text{ g L}^{-1}$, respectively, while a 100% RE_{settler} was recorded (Table 3). The C, N and P biomass content during stage III was 38.5%, 6.5% and 1.4%, respectively (Table 4). *Synechocystis aquatilis* was the predominant microalga in this period, with *Microspora* sp. and *Pseudanabaena minima* present at similar proportions. The lipid content increased to $8.9\pm 3.2\%$ during stage III, which constituted the maximum value recorded.

An increase in the liquid recirculation from 1.1 to $3.5 \text{ m}^3 \text{ m}^{-2} \text{ h}^{-1}$ in stage IV (corresponding to a L/G increase in the AC from 0.9 to 2.9) resulted in an enhancement in RE_{CO_2} up to $84\pm 4\%$ without increase in the O_2 concentration in the upgraded biogas (Fig. 4).

Figure 4

Despite RE_{CO_2} increased, RE_C remained similar to previous stage ($19\pm 3\%$), which caused an IC concentration increase to $222\pm 15 \text{ mg L}^{-1}$. RE_{TN} increased to $57\pm 3\%$, while RE_{P_s} and P_s concentration were similar to stage III ($45\pm 10\%$ and $1.7\pm 0.5 \text{ mg L}^{-1}$, respectively). The biomass productivity and TSS concentration in the HRAP during stage IV slightly decreased to $3.4\pm 0.2 \text{ g m}^{-2} \text{ d}^{-1}$ and $0.22\pm 0.01 \text{ g L}^{-1}$, respectively, with a RE_{settler} of $95.5\pm 1.5\%$ (Table 3). The C, N and P biomass composition was similar to previous stages (40.1%, 7.1% and 1.3%, respectively). *Synechocystis aquatilis* (67%) was again the predominant microalgae. *Microspora* sp. almost disappeared, while *Pseudanabaena minima* increased its predominance to 33% of cells (Fig. 3). The lipid content decreased to $4.1\pm 1.0\%$.

Centrate dilution was increased to 1:70 during stage V in order to induce the nitrogen starvation conditions required for lipid accumulation. RE_{CO_2} , RE_C and IC concentrations of $82\pm 2\%$, $22\pm 1\%$ and $211\pm 6 \text{ mg L}^{-1}$, respectively, were recorded. The lower nutrient load implied an increase in RE_{TN} to $70\pm 6\%$ and a decrease in the effluent TN concentration to 5 mg N L^{-1} . Similarly, RE_{P_s} increased to $53\pm 12\%$ with a concomitant decrease in P_s effluent concentration to $0.7\pm 0.1 \text{ mg L}^{-1}$. Despite the lower nutrient load applied, biomass productivity and TSS concentration remained similar at $4.4\pm 1.0 \text{ g m}^{-2} \text{ d}^{-1}$ and $0.29\pm 0.03 \text{ g L}^{-1}$, respectively, with a complete biomass removal in the settler (Table 3). Similarly to previous operational stages, the C, N and P biomass composition was 42.5%, 6.2% and 1.6%, respectively. *Pseudanabaena minima* was identified as the dominant taxon (92% of cells). A slightly higher lipid content of $7.4\pm 0.4 \%$ was achieved during stage V (Table 4).

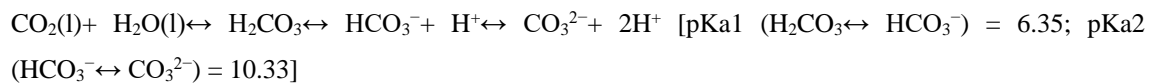
The increase in the external liquid recirculation to $9.9 \text{ m}^3 \text{ m}^{-2} \text{ h}^{-1}$ (L/G of 8.3 in the AC) in stage VI resulted in RE_{CO_2} up to $99\pm 0\%$, and entailed an increase in the O_2 concentration of the upgraded biogas

from $2.1 \pm 1.2\%$ to $20.7 \pm 0.1\%$ (Fig. 4). Despite a slightly high increase in RE_C to $27 \pm 6\%$ was recorded, the IC concentration in the effluent increased to $228 \pm 15 \text{ mg L}^{-1}$. A complete TN removal was achieved in stage VI, which supported the occurrence of nitrogen deprivation conditions. Likewise, the high RE_{Ps} ($82 \pm 3\%$) recorded resulted in the lowest $P\text{-PO}_4^{3-}$ concentrations in the HRAP (0.2 mg L^{-1}). Biomass productivity and TSS concentration remained at $3.6 \pm 0.1 \text{ g m}^{-2} \text{ d}^{-1}$ and $0.23 \pm 0.02 \text{ g L}^{-1}$, respectively, with a RE_{settler} of 97% (Table 4). C, N and P composition corresponded to 43.6%, 7.5% and 1.4%, respectively. Finally, microalgae population during stage VI was characterized by a high biodiversity. Despite *Limnothrix mirabilis* was the dominant species (57%), *Geitlerinema* sp., *Synechocystis aquatilis* and *Woronichinia* sp. were present at similar cell proportions ($\approx 12\text{-}15\%$). The lipid content of the algal-bacterial biomass decreased to $3.3 \pm 0.7\%$, which represented the lowest recorded value.

Discussion

Evaporation rate in the HRAP was similar to outdoors systems ($\approx 2\text{-}7 \text{ L m}^{-2} \text{ d}^{-1}$ depending on the geographical area and the HRAP operational conditions; Guieysse et al. 2013; Murphy and Allen 2011) due to the high turbulence in the pond mediated by motor oversizing typical of lab or pilot scale systems (Mendoza et al. 2013). This high cultivation broth turbulence, together with the *in-situ* O_2 produced by microalgae, maintained DO at $6\text{-}8 \text{ mg L}^{-1}$, well above the O_2 half saturation constant for organic matter oxidation and nitrification ($\geq 2 \text{ mg O}_2 \text{ L}^{-1}$) (Metcalf and Eddy 2003). Likewise, this high turbulence avoided that algal cells remained long periods of time in the dark.

The estimated dissolved CO_2 concentration in the liquid phase was calculated based on the pH and IC concentration in the cultivation broth of the HRAP and on the CO_2 aqueous equilibrium (Metcalf and Eddy, 2003):



According to these calculations, the estimated dissolved CO_2 concentration in the liquid phase decreased from 0.44 (stage I) to approximately 0.03 mg L^{-1} when the pH was increased to 9.5 in stage II. This tiny decrease in the dissolved CO_2 concentration in the bulk aqueous phase when pH was increased did not result in significant enhancements in the CO_2 concentration gradient from the CO_2 aqueous equilibrium in the column (the CO_2 gradient increased from $433.6 \pm 9.3 \text{ mg L}^{-1}$ to $434.0 \pm 8.2 \text{ mg L}^{-1}$) and consequently in RE_{CO_2} in the CO_2 -AC (Fig. 5a/5b). The estimated CO_2 equilibrium concentration in the liquid phase in the AC was calculated using the ideal gas equation and a Henry's adimensional constant of 0.83 at 20°C (Sander, 1999), which resulted in a CO_2 equilibrium concentration of $\approx 434 \text{ mg CO}_2 \text{ L}^{-1}$ (Fig. 5a/5b). Similarly, the decrease in the diffuser pore size (which entailed higher gas-liquid interfacial areas), did not result in enhancements of RE_{CO_2} due to the higher influence of the liquid recirculation flow rate on CO_2 removal as discussed below. In this context, the superior biogas upgrading at higher external liquid recirculation rates was likely due to the higher net CO_2 absorption in the algal-bacterial recycling broth since CO_2 mass transfer to the aqueous phase did not limit the upgrading process during stages I to III. On the other hand, the oxygen content in the upgraded biogas increased at increasing the liquid recirculation rate above $3.5 \text{ m}^3 \text{ m}^{-2} \text{ h}^{-1}$, at concentrations well above regulatory limits in most European legislations for biomethane injection in natural gas grids ($\leq 0.3\%$) (BOE 2013). This high O_2 content in the biogas at stage

VI would entail potential explosion hazards. In this context, the presence of high H₂S concentrations in the biogas and its rapid oxidation in the absorption column, together with the application of further operational strategies in this innovative biogas upgrading technology (e. g. feeding raw centrate or wastewater to the AC to deplete the O₂ present in the microalgal recycling stream via organic matter mineralization), are expected to lower these O₂ concentrations (Bahr et al. 2014; Serejo et al., 2015). The almost complete removal of CO₂ (99±0%) at a L/G ratio of 8.3 was higher than the RE_{CO₂} reported by Serejo et al. (2015) (≈80%) at a L/G ratio of 10, which was determined as the optimum to achieve 100% of H₂S removal and O₂ concentrations in the treated biogas of ≈1%. In addition, it must be highlighted that the energy cost associated to the external recirculation was negligible compared to the energy requirements for mixing in the HRAPs (Bahr et al. 2014). Finally, it should be stressed that solubilization and biological oxidation of CH₄ would be expected when upgrading real biogas. However, preliminary tests carried out in our laboratory with simulated biogas showed average CH₄ losses of ≈ 1% (on mass basis) and a negligible effect of CH₄ on algal population activity (Serejo et al., 2015).

Figure 5

The main causes underlying the negative RE_{STOC} recorded during the six operational stages were the low concentration and poor biodegradability of the dissolved organic carbon in the diluted centrates fed to the HRAP (Table 1) and the likely presence of TOC released by microalgal metabolism or TOC corresponding to biomass lysis (Posadas et al. 2013; Bahr et al., 2014; Dong et al., 2014; Serejo et al., 2015). At this point it should be stressed that any photosynthetic biogas-upgrading system is a net bioconverter of dissolved inorganic carbon into particulate organic carbon, and the active lysis of this structural organic carbon (often 10-15 % of the new microalgae biomass produced) generates significant amounts of dissolved recalcitrant organic carbon in the form of algal cell debris. On the other hand, the positive CO₂ concentration gradient established between the bulk liquid phase (CO_{2(l)} = 0.44 mg CO₂ L⁻¹) and the atmosphere (CO_{2*(l)} = 0.38 mg CO₂ L⁻¹) promoted CO₂ removal by stripping in stage I, since only 17±6% of the total carbon removed was recovered in the harvested biomass. The estimated aqueous CO₂ concentration in equilibrium with the atmosphere was also calculated using the ideal gas equation and a Henry's adimensional constant of 0.83 at 20°C (Sander, 1999), which resulted in an equilibrium concentration of ≈0.38 mg CO₂ L⁻¹ (Fig. 5c/5d). However, the high pH value imposed from stage II onward compared to the reported optimum values of 8 for algal growth of 7-9 for wastewater treatment in HRAPs (Acién et al., 2012; Posadas et al., 2015) mediated CO₂ absorption from the atmosphere (CO_{2(l)} ≈0.03 mg CO₂ L⁻¹ from stage II onwards) and prevented CO₂ removal by stripping, despite the higher IC concentrations present in the cultivation broth (Fig. 5c/5d). Indeed, the total carbon recovered in the harvested biomass from stage II onward accounted for 100±5% of the total C removed in the HRAP.

TN during stage I was removed by assimilation into biomass (15±8%) and by N-NH₄⁺ stripping (Cai et al. 2013; De Godos et al. 2009). Despite pH was increased to 9.5 from stage II onward, 85±2% of the TN removed was recovered in the harvested biomass. In this context, the complete N-NH₄⁺ removal and the high nitrification activity supported by the high N-NO₃⁻ effluent concentrations at all operational stage (Table 3), indicated that N-NH₄⁺ oxidation by nitrifying bacteria was faster than N-NH₄⁺ volatilization. Similar results were obtained when treating raw domestic wastewater in an algal turf scrubber

photobioreactor at HRTs of 5-10d (Posadas et al. 2013). As a matter of fact, the RE_{TN} decrease during stages II and III was correlated to the increase in $N-NO_3^-$ concentration (which prevented NH_4^+ volatilization). On the other hand, the higher IC availability could have mediated the slight increase in TN removal as a result of an enhanced biomass growth at stage IV, while the lower N loads supplied from stage V onward resulted in the higher RE_{TN} recorded. An increase in nitrification activity as a result of the higher IC availability was ruled out based on the steady decrease in nitrate concentration from stage IV onward.

RE_{P_s} also showed a significant increase compared to stages II, III and IV when centrate dilution was increased. Phosphorus assimilation into biomass was the main removal mechanism during the six operational stages, with $98\pm 3\%$ of the total removed P_s recovered in the harvested biomass (Cai et al. 2013). Phosphorus did not limit microalgae growth, which occurs at P_s concentrations below 0.2 mg L^{-1} .

The fact that the increase in RE_{CO_2} did not result in higher biomass productivities was caused by the low nutrient loads fed into the system in order to increase biomass lipid content. Thus, these biomass productivities (maximum productivity of $5.4\pm 0.2 \text{ g m}^{-2} \text{ d}^{-1}$ in stage II), which could be increased by increasing the nutrient loads, were significantly lower than the typical productivities reported in outdoors HRAPs ($\approx 15-20 \text{ g m}^{-2} \text{ d}^{-1}$) (Chisti 2007). Nitrogen deprivation was the selected strategy to increase microalgae lipid content, which resulted in the low biomass productivities recorded. However, a balance between biomass lipid content and biomass productivity should be targeted in real scale applications (Feng et al., 2011). The enhanced biomass settleability ($\approx 100\% RE_{\text{settler}}$) achieved at the highest biomass concentrations ($\geq 0.22 \text{ g TSS L}^{-1}$) were in agreement with the findings of Park et al. (2011b). In this context, microalgae-based wastewater treatment with effective biomass harvesting by settling represent a cost-effective alternative for algal biomass reutilization compared to conventional physical-chemical techniques such as centrifugation or coagulation/flocculation (De Godos et al. 2011).

Similar C, N and P biomass contents were recorded during the 225 d of experimentation regardless of the different C and nutrient load applied, which confirms the constant composition of the algal-bacterial biomass cultivated in wastewater (Posadas et al. 2013). The C, N and P biomass contents were in agreement with those reported by Dominguez-Cabanelas et al. (2013) (C: 43-56%; N:2-9%; P: 1.4%).

A high microalgae biodiversity was found regardless of the operational conditions tested. However, no significant correlation between cultivation conditions and the predominant microalgae species was clearly elucidated. The open design of the HRAP, together with the variations in characteristics of the fed diluted centrate, likely explained the high biodiversity and the rapid changes in the population structure (Devi et al. 2012). These results confirmed the difficulty to maintain monoalgal species in open photobioreactors treating wastewaters (De Godos et al. 2009; García et al. 2000; Serejo et al., 2015).

The lipid content of the algal-bacterial biomass remained low despite the different carbon and nutrient supply strategies evaluated. The lipid contents obtained (2.9 -11.2%) were in the low reported range in axenic microalgae cultures (5-77%, Chisti 2007), but were similar to those values reported in microalgae cultivated in wastewaters (2-23%, Serejo et al., 2015; Sepúlveda et al., 2015). Contrary to previous findings (Toledo-Cervantes et al. 2013), nitrogen depletion in stages I and VI did not result in higher

biomass lipid contents. The higher carbon availability during stages II and III compared to the start-up period likely resulted in an increase in biomass lipid content. Unfortunately, these contents were not sufficient to sustain a cost-effective wastewater to biodiesel process ($\approx 30\text{-}40\%$; Chisti 2007). This might be explained by the fact that only few of the species found in the HRAP are lipid producers in moderate contents. In this context, despite *Scenedesmus* sp. has been reported as the most efficient producer of lipids suitable for biodiesel among the identified microalgae, its abundance in the HRAP was low and only limited to stage I (Mandal and Mallick 2012). The low light irradiances could have also contributed to the poor biomass lipid accumulation in this preliminary proof of concept study under nutrient limitation, since some authors have reported an enhanced lipid synthesis at increasing light irradiances (without reaching photosaturation conditions) under nitrogen limited microalgae growth (Klok et al. 2013; Kandilian et al., 2014). In this context, the biomass here harvested could be used for other purposes than for biodiesel production. Among the potential uses of this residual algal biomass are biofertilization, feedstock for the production of bioethanol and/or biogas (depending on its respective protein and carbohydrate contents) (Romero García et al., 2012; Hernández et al., 2015; Collet et al., 2011; Wang et al., 2013). Despite the natural variation of solar irradiation, n° of sun hours and temperature is likely to hinder a fair comparison among the different experimental stages, a further evaluation of this technology must be carried out under outdoors conditions based on the promising results for biogas upgrading and wastewater treatment here reported.

In brief, a complete CO₂ removal from biogas was achieved at liquid recirculation rates of $9.9 \text{ m}^3\text{m}^{-2}\text{h}^{-1}$, which confirms the potential of this technology to photosynthetically upgrade biogas based on residual nutrients from anaerobic digesters. Assimilation into biomass represented the main N and P removal mechanisms at pH 9.5 regardless of the operational conditions. Biomass composition remained constant despite the rapid dynamics in microalgae population structure. The HRAP also supported an efficient biomass-effluent separation by settling ($>95\%$). Finally, the low lipid content (2.9-11.2%) recorded throughout the different operational stages (even under nutrient limitation), showed the technical difficulty of developing cost-effective wastewater treatment to biodiesel processes and the harvested biomass could be applied for other profitably uses such as biofertilizers or bioethanol and biogas production.

REFERENCES

- Ación FG, Fernández JM, Magán JJ, Molina E (2012) Production cost of a real microalgae production plant and strategies to reduce it. *Biotechnol Adv* 30:1344-1353
- Alam F, Date A, Rasjidin R, Mobin S, Moria H, Baqui A (2012) Biofuel from algae-Is it a viable alternative? *Procedia Engineering* 49:221-227 DOI:10.1016/j.proeng.2012.10.131

- Arbib Z, Ruiz J, Álvarez-Díaz P, Garrido-Pérez C, Barragán J, Perales JA (2013) Effect of pH control by means of flue gas addition on three different photo-bioreactors treating urban wastewater in long-term operation. *Ecol Eng* 57:226-235 DOI:10.1016/j.ecoleng.2013.04.040
- Bahr M, Díaz I, Domínguez A, González-Sánchez A, Muñoz R (2014) Microalgal-biotechnology as a platform for an integral biogas upgrading and nutrient removal from anaerobic effluents. *Environ Sci Technol* 48:573-581
- Bird RB, Stewart W, Lightfoot EN (2006) *Transport Phenomena*. 2nd Edition. Ed. Limusa.
- BOE (Boletín oficial del Estado), 2013. https://www.boe.es/diario_boe/txt.php?id=BOE-A-2013-185 (Last accessed: 22.09.2014)
- Breuer G, Lamers PP, Martens DE, Draaisma RB, Wijffels RH (2012) The impact of nitrogen starvation on the dynamics of triacylglycerol accumulation in nine microalgae strains. *Bioresour Technol* 124: 217-226
- Cai T, Park SY, Li Y (2013) Nutrient recovery from wastewater streams by microalgae: Status and prospects. *Renew. Sust Energ Rev* 19:360-369 DOI:10.1016/j.rser.2012.11.030
- Chisti Y (2007) Biodiesel from microalgae. *Biotechnol Adv* 25:294-306
- Christenson L, Sims R. (2011) Production and harvesting of microalgae for wastewater treatment, biofuels and bioproducts. *Biotechnol Adv* 29:686-702
- Collet P, Hélias A, Lardon L, Ras M, Goy R A, Steve J P (2011) Life-cycle assessment of microalgae culture coupled to biogas production. *Bioresour Technol* 102:207-214
- De Godos I, Blanco S, García-Encina PA, Becares E, Muñoz R (2009) Long-term operation of high rate algal ponds for the bioremediation of piggery wastewaters at high loading rates. *Bioresour Technol* 100:4332-4339 DOI:10.1016/j.biortech.2009.04.016
- De Godos I, Guzmán HO, Soto R, García-Encina P, Becares E, Muñoz R, Vargas VA (2011) Coagulation/flocculation-based removal of algal-bacterial biomass from piggery wastewater treatment. *Bioresour Technol* 102:923-927
- Devi MP, Swamy YV, Mohan SV (2013) Nutritional mode influences lipid accumulation in microalgae with the function of carbon sequestration and nutrients supplementation. *Bioresour Technol* 142:278-286 DOI:10.1016/j.biortech.2013.05.001
- Dominguez Cabanelas IT, Ruiz J, Arbib Z, Alexandre C, Garrido-Pérez C, Rogalla F, Nascimiento IA, Perales JA (2013) Comparing the use of different domestic wastewaters for coupling microalgal production and nutrient removal. *Bioresour Technol* 131:429-436 DOI:10.1016/j.biortech.2012.12.152
- Dong B, Ho N, Ogden K, Arnold R G (2014) Cultivation of *Nannochloropsis salina* in municipal wastewater or digester centrate. *Ecotox Environ Safe* 103:45-53
- Eaton AD, Clesceri LS, Greenberg AE (2005) *Standard methods for the examination of water and wastewater*. 21 st edition. American Public Health Association/American Water Works Association/ Water Environment Federation
- Feng D, Chen Z, Xue S, Zhang W (2011) Increased lipid production of the marine oleaginous microalgae *Isochrysis zhangjiangensis* (Chrysophyta) by nitrogen supplement. *Bioresour Technol* 102:6710-6716

- García J, Hernández MM, Mujeriego R (2000) Influence of phytoplankton composition on biomass removal from high-rate oxidation lagoons by means of sedimentation and spontaneous flocculation. *Water Environ Res* 72:230-237
- González C, Marciniak J, Villaverde S, García-Encina PA, Muñoz R (2008) Microalgae-based processes for the biodegradation of pretreated piggery wastewaters. *Appl Microbiol Biotechnol* 80:891-898
- Guieysse B, Béchet Q, Shilton A (2013) Variability and uncertainty in water demand and water footprint assessments of fresh algae cultivation based on case studies from five climatic regions. *Bioresour Technol* 128:317-323
- Hernández D, Riaño B, Coca M, García-González M C (2015) Saccharification of carbohydrates in microalgal biomass by physical, chemical and enzymatic pre-treatments as a previous step for bioethanol production. *Chem Eng J* 262:939-945 DOI:10.1016/j.cej.2014.10.049
- Heubeck S, Craggs R J, Shilton A (2007) Influence of CO₂ scrubbing from biogas on the treatment performance of a high rate algal pond. *Water Sci Technol* 55 (11):193-200
- Kandilian R, Pruvost J, Legrand J, Pilon L (2014) Influence of light absorption rate by *Nannochloropsis oculata* on triglyceride production during nitrogen starvation. *Bioresour Technol* 163:308-319
- Klok AJ, Martens DE, Wijffels R, Lamers PP (2013) Simultaneous growth and neutral lipid accumulation in microalgae. *Bioresour Technol* 134:233-243
- Kochert G (1978) *Handbook of phycological methods*. London: Cambridge University Press
- Mandal S, Mallick N (2012) Biodiesel Production by the Green Microalga *Scenedesmus obliquus* in a Recirculatory Aquaculture System. *Appl Environ Microbiol* 78(16):5929–5934
- Mendoza JL, Granados MR, De Godos I, Ación FG, Molina E, Banks C, Heaven S (2013) Fluid-dynamic characterization of real scale raceway reactors for microalgae production. *Biomass Bioenerg* 54: 267-275 DOI:10.1016/j.biombioe.2013.03.017
- Metcalf, Eddy (2003) *Wastewater Engineering and Reuse*, 4th ed., New York, Mc. Graw Hill
- Muñoz R, Guieysse B (2006) Algal-bacterial processes for the treatment of hazardous contaminants: a review. *Water Res* 40:2799-2815
- Murphy CF, Allen DT (2011) Energy-water nexus for mass cultivation of algae. *Environ Sci Technol* 45: 5861-5868
- Norsker NH, Barbosa MJ, Vermuë MH, Wijffels RH (2011) Microalgal production: a close look at the economics. *Biotechnol Adv* 29: 24–27
- Park JBK, Craggs RJ, Shilton AN (2011) Wastewater treatment high rate algal ponds for biofuel production. *Bioresour Technol* 102:35-42
- Park JBK, Craggs RJ, Shilton AN (2011b) Recycling algae to improve species control and harvest efficiency from a high rate algal pond. *Water Res* 45(20): 6637-6649
- Posadas E, García-Encina PA, Soltau A, Domínguez A, Díaz I, Muñoz R. (2013) Carbon and nutrient removal from centrates and domestic wastewater using algal-bacterial biofilm bioreactors. *Bioresour Technol* 139:50-58
- Posadas E, Morales MM, Gómez C, Ación FG, Muñoz R (2015) Influence of pH and CO₂ source on the performance of microalgae-based secondary domestic wastewater treatment in outdoors pilot raceways. *Chem Eng J* 265:239-248 DOI:10.1016/j.cej.2014.12.059

- Romero García J M, Guzmán J L, Moreno J C, FernándezSevilla J M (2012) Filtered Smith Predictor to control pH during enzymatic hydrolysis of microalgae to produce L-aminoacids concentrates. *Chem Eng Sci* 82:121-131
- Sander R (1999) Compilation of Henry's Law Constants for Inorganic and Organic Species of Potential Importance in Environmental Chemistry; <http://www.mpch-mainz.mpg.de/~sander/res/henry.html>, 1999. (Last accessed: 20.03.2015)
- Sepúlveda C, Acién F G, Gómez C, Jiménez Ruiz N, Riquelme C, Molina-Grima E (2015) Utilization of centrate for the production of the marine microalgae *Nannochloropsis gaditana*. *Algal Res* 9:107-116 DOI:10.1016/j.algal.2015.03.004
- Serejo M L, Posadas E, Boncz M A, Blanco S, García-Encina P A, Muñoz R (2015) Influence of biogas flow rate on biomass composition during the optimization of biogas upgrading in microalgal-bacterial processes. *Env Sci Technol* 49 (50): 3228-3236
- Shriwastav A, Bose P (2015) Algal growth in photo-bioreactors: Impact of illumination strategy and nutrient availability. *Ecol Eng* 77:202-215 DOI: 10.1016/j.ecoleng.2015.01.034
- Sournia A (1978) *Phytoplankton Manual*. Museum National d' Historie Naturelle, Paris. United Nations Educational, Scientific and Cultural Organization (Unesco)
- Toledo-Cervantes A, Morales M, Novelo E, Revah S (2013) Carbon dioxide fixation and lipid storage by *Scenedesmus obtusiusculus*. *Bioresour Technol* 130:652-658
- Wang X, Nordlander E, Thorin E, Yan J (2013) Microalgal biomethane production integrated in an existing biogas plant: A case study in Sweden. *Appl Energ* 112:478-484 DOI: 10.1016/j.apenergy.2013.04.087

FIGURE CAPTIONS

Figure 1. Schematic diagram of the continuous biogas upgrading and nutrient removal experimental set-up. Grey circles represent liquid sampling ports (1: influent, 2: effluent; 3: cultivation broth) and grey squares represent gas sampling ports (1: inlet biogas, 2: upgraded biogas). Continuous lines represent liquid streams and dashed lines represent biogas streams.

Figure 2. Time course of CO₂ removal in the absorption column (○) and IC concentration in the cultivation broth (●).

Figure 3. Time course of the microalgae population structure in the HRAP during the six operational stages.  *Chroococidiopsis* sp.,  *Cyanosarcina* sp.,  *Geitlerinema* sp.,  *Limnothrix mirabilis*,  *Microspora* sp.,  *Mucidosphaerium pulchellum*,  *Pseudanabaena minima*,  *Scenedesmus* sp.,  *Synechocystis aquatilis* and  *Woronichinia* sp.

Figure 4. Influence of the liquid recirculation flow rate in the CO₂-AC on CO₂ removal (continuous line) and O₂ concentration in the upgraded biogas (discontinuous line).

Figure 5. Estimated CO₂ concentration gradients between the biogas and the external recirculating cultivation broth in the AC at a pH of 8.5 (a) and 9.5 (b), and between the cultivation broth in the HRAP and the atmosphere at a pH of 8.5 (c) and 9.5 (d).

Figure 1

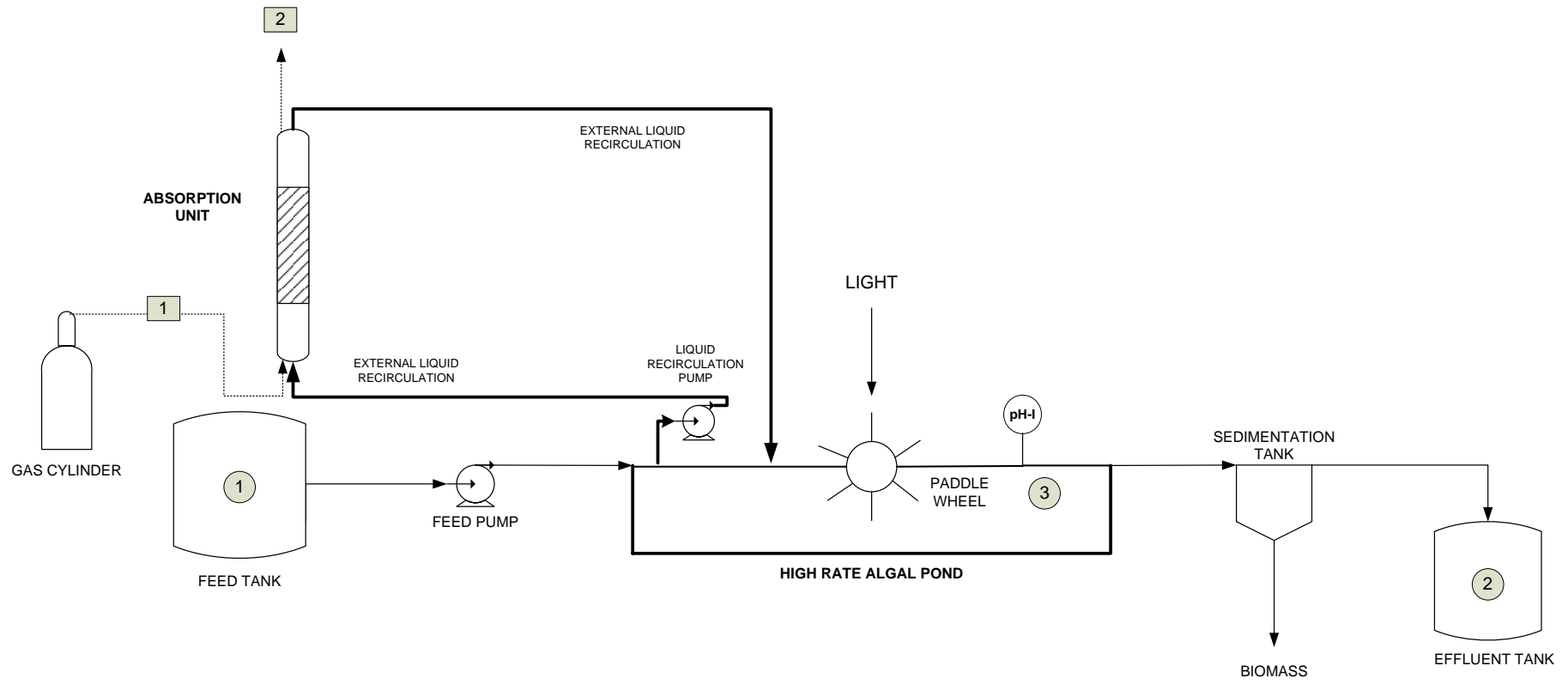


Figure 2

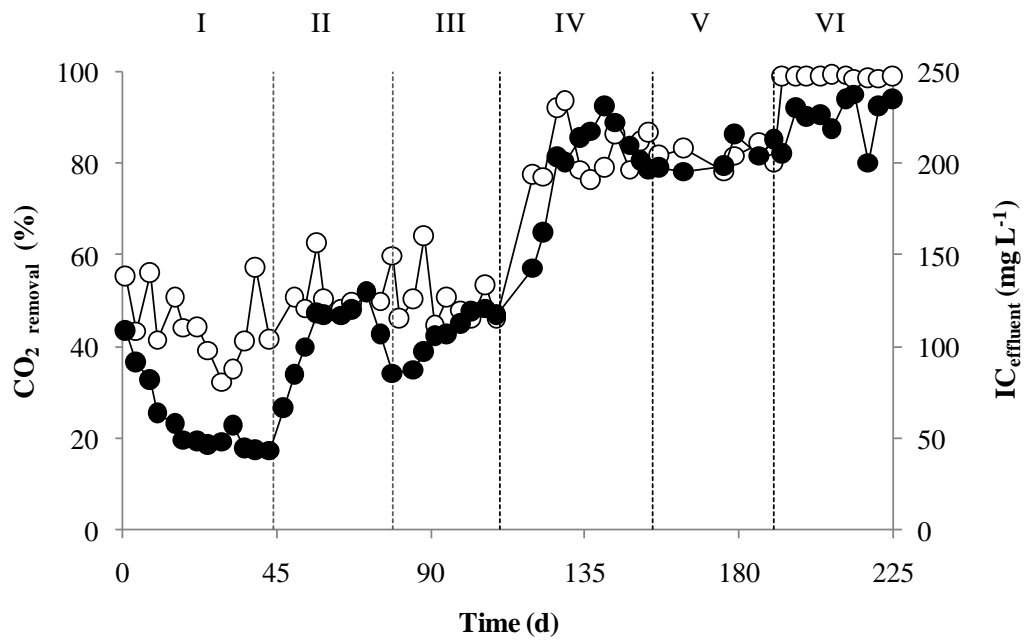


Figure 3

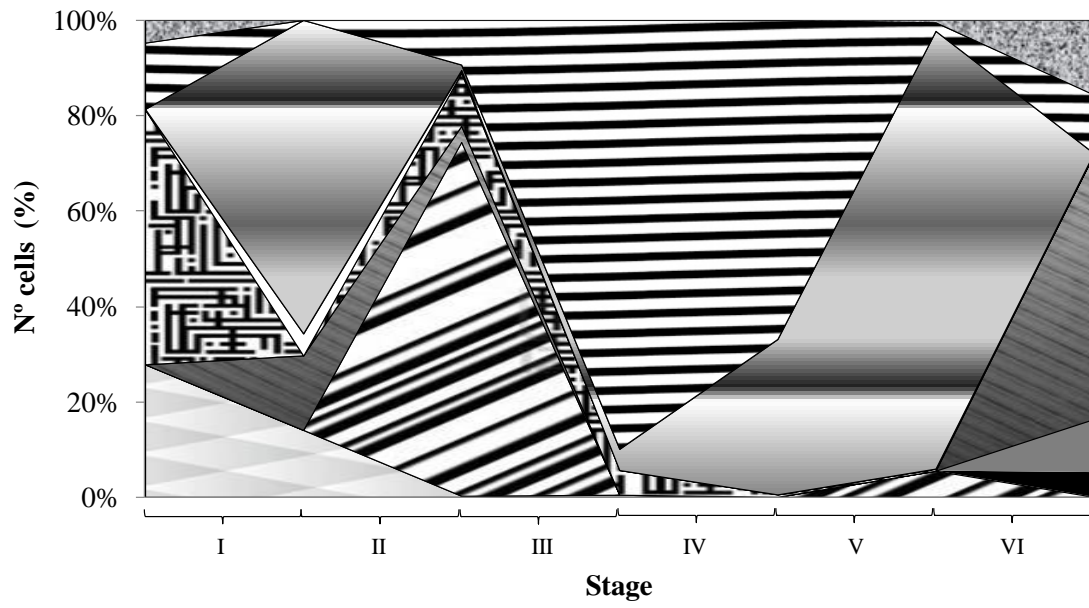


Figure 4

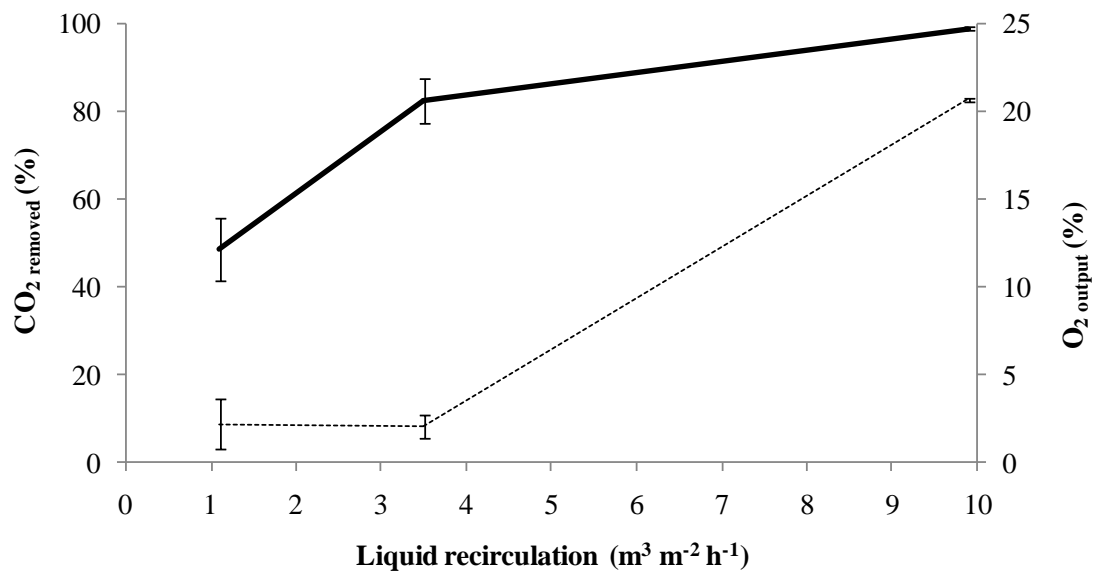


Figure 5

